



Research articles

Emission of electromagnetic radiation due to spin-flip transitions in a ferromagnet

E.A. Karashtin*

Institute for physics of microstructure of RAS, Nizhniy Novgorod, 603950, GSP-105, Russia
Lobachevsky University, Gagarin ave., 23, Nizhniy Novgorod, 603950, Russia

ARTICLE INFO

Keywords:

Exchange interaction
Spin-orbit coupling
Non-collinear ferromagnet
Tunnel magnetic junction

ABSTRACT

We theoretically analyze the probability of electromagnetic wave emission due to electron transitions between spin subbands in a ferromagnet. Different mechanisms of such spin-flip transitions are considered. One mechanism is electron transitions caused by the magnetic field of the wave. Another mechanism is due to the Rashba spin-orbit interaction. While the two mentioned mechanisms contribute in a homogeneously magnetized ferromagnet, there are two other mechanisms that occur for a non-collinearly magnetized medium. The first mechanism is known and is due to the dependence of the exchange interaction constant on the quasimomentum of the conduction electrons. The second one is due to the minimal coupling. It follows from the connection of spin and spatial degrees of freedom in any non-collinearly magnetized medium. We study these mechanisms in a non-collinear ferromagnet with a helicoidal magnetization distribution. Estimations of the probabilities of electron transitions due to different mechanisms are made for realistic parameters, and we compare the mechanisms. We also estimate the radiation power and the threshold current in a simple model in which spin is injected into the ferromagnet by a spin-polarized electric current through a tunnel barrier.

1. Introduction

Electron transitions between energy bands may be accompanied by electromagnetic wave generation. This paper is devoted to the mentioned phenomenon when electrons jump between spin subbands in a ferromagnet. In a simple conductor without a spin-orbit interaction or applied magnetic field the energy states of conduction electrons are doubly degenerate with respect to spin. In a homogeneous ferromagnet their spin states are split into two subbands. The energy gap between these subbands usually corresponds to an infrared or terahertz frequency, depending on the material [1,2]. Therefore study of electron transitions between the spin subbands by electromagnetic wave generation is important. This is encouraged by a possibility of precise control of the magnetic state of the ferromagnet by applying a magnetic field or fabrication of different nanostructures [3–9].

Terahertz wave generation by ferromagnets which are irradiated by a femtosecond optical pulse was developed recently [10–14]. Usually this effect is explained by intraband electron transitions, i.e. processes without spin flip [15]. The terahertz frequency range follows from the pulse duration (typically it is 10–50 fs which corresponds to 20–100 THz). The emission spectrum here is characterized by broad frequency range. Considering the interband electron transitions, i.e. transitions with spin flip, the frequency range is determined by the energy

gap between spin subbands. Further, stimulated emission of electromagnetic wave may be obtained in such case.

It is well known that electric-dipole transitions of electrons between spin subbands are forbidden in a homogeneous ferromagnet. In order to show this, let us consider the Vonsovsky s-d exchange model [16]. In this model, the magnetization \mathbf{M} is created by localized d- or f-electrons, and the conduction electrons which are supposed to be s-electrons have the following hamiltonian:

$$\hat{H} = \frac{\hat{p}^2}{2m_e} + J(\hat{\sigma} \cdot \mathbf{M}), \quad (1)$$

where $\hat{p} = -i\hbar\nabla$ is the electron momentum operator, m_e is the electron mass, J is the exchange constant, $\hat{\sigma}$ is the vector of Pauli matrices which is proportional to the operator of electron spin. Here \mathbf{M} is supposed to be a constant vector along the Cartesian z-axis. In equilibrium, the electron wavefunctions are

$$\psi_+ = \exp(i\mathbf{k}\mathbf{r}) \begin{pmatrix} 1 \\ 0 \end{pmatrix}, \psi_- = \exp(i\mathbf{k}\mathbf{r}) \begin{pmatrix} 0 \\ 1 \end{pmatrix}, \quad (2)$$

where \mathbf{k} is the electron wave vector, \mathbf{r} is the vector of Cartesian coordinates. The wave functions of two spin subbands correspond to electrons with average spin either parallel or antiparallel to \mathbf{M} .

* Correspondence to: Institute for physics of microstructure of RAS, Nizhniy Novgorod, 603950, GSP-105, Russia.
E-mail address: eugenk@ipmras.ru.

These wavefunctions are orthogonal to each other. In the electro-dipole approximation, only the electric field of the wave $\mathbf{E}_\omega = \mathbf{E} \exp(-i\omega t)$ is taken into account (ω is the wave frequency). The coordinate dependence of this electric field leads to spatial dispersion. It should be neglected in the electric dipole approximation (the corrections brought about by the wave spatial dispersion are usually very small). In order to study the interaction of electrons with an electromagnetic wave in such approximation, it is convenient to take the gauge for which the electric potential is zero. Thus the electron momentum operator \hat{p} should be changed to $(\hat{p} - \frac{e}{c} \mathbf{A}_\omega)$ [17,18], where $\mathbf{A}_\omega = -i \frac{c}{\omega} \mathbf{E}_\omega$ is the vector-potential. The operator of interaction of electrons and electromagnetic wave takes the form

$$\hat{H}_{mc}^\omega = \frac{e\hbar}{2m_e c \omega} (\mathbf{E}_\omega \cdot \nabla), \quad (3)$$

where e is the absolute electron charge. This interaction is called the minimal coupling [19]. It is obvious that since the operator (3) does not change the electron spin its matrix element is zero and thus the electron transition probability due to interaction with an electromagnetic wave is zero.

This situation can be changed by taking into account some additional interaction or condition that breaks such symmetry. It was predicted earlier that if the exchange constant depends on the electron momentum $J = J(\hat{p})$ the electron transitions are allowed [20,21]. In order to obtain these transitions, one should take into account that the electron momentum should be shifted here due to non-zero \mathbf{A}_ω , as in (1). This leads to an additional operator for the interaction of the electron and the electromagnetic wave linear in \mathbf{E}_ω

$$\hat{H}_J^\omega = -i \frac{e}{\omega} \left(\mathbf{E}_\omega \cdot \frac{\partial J}{\partial \mathbf{p}} \right) (\hat{\sigma} \cdot \mathbf{M}). \quad (4)$$

The interaction operator (4) flips spins in the case of a non-collinearly magnetized medium and therefore leads to electron transitions. This mechanism of electromagnetic wave emission has been studied previously [22,23] in a system that consists of two magnetic layers in which the magnetizations are not parallel. Experiments on electromagnetic wave generation in non-uniform ferromagnets were performed inspired by these investigations [24–26]. Additional modifications such as anisotropic exchange interaction were considered in order to improve the wave generation properties [27]. However it is hard to separate the mentioned mechanism from others that are possible in the existing experiments. Another important property of this mechanism is its spin–orbit nature. Indeed, only the exchange interaction is taken into account in the hamiltonian (1). But the dependence of J on electron momentum may arise only from the spin–orbit interaction in the subsystem of localized d- or f-electrons.

There are mechanisms of electron spin-flip transitions in ferromagnets different from the one described in the previous paragraph. The most simple mechanism is caused by the magnetic field of the wave. The magnetic field provides transitions through the Zeeman interaction [17]

$$\hat{H}_Z^\omega = \mu_0 g (\hat{\sigma} \cdot \mathbf{B}_\omega) \quad (5)$$

where \mathbf{B}_ω is the magnetic field of the wave, g is the electron g-factor that is supposed to be equal to 2, μ_0 is the Bohr magneton. Another mechanism that exists in homogeneously magnetized ferromagnet is caused by the spin–orbit interaction. In this paper the Rashba coupling [19,28] is considered

$$\hat{H}_R = i (\boldsymbol{\alpha}_R \cdot [\nabla \times \hat{\sigma}]). \quad (6)$$

It usually appears at surfaces, and the Rashba vector $\boldsymbol{\alpha}_R$ is parallel to the surface normal and leads to the interaction of electrons with the electromagnetic wave in the form (for details, see appropriate section below):

$$\hat{H}_R^\omega = \frac{ie}{2\hbar\omega} (\boldsymbol{\alpha}_R \cdot [\hat{\sigma} \times \mathbf{E}_\omega]). \quad (7)$$

Finally, a fully exchange mechanism exists in non-collinearly magnetized ferromagnets due to the connection between spin and spatial coordinates in such ferromagnets. This mechanism follows from the interaction hamiltonian (3) which should be applied to the mixed spin states of a non-collinear ferromagnet. It was theoretically demonstrated recently [29] and is studied insufficiently.

In the present work, we consider the magnetic helicoid (Bloch type spiral):

$$\mathbf{M} = e_x \cos qz + e_y \sin qz, \quad (8)$$

where q is inversely proportional to the spiral step, and the Cartesian coordinate system with the z -axis along the spiral axis is chosen. This type of magnetization structure is realized for example in holmium [30] and in manganese silicene [31] at low temperature. In holmium material, electromagnetic wave absorption with spin flip electron transitions is known [2,32]. This phenomenon is inverse to the electromagnetic wave generation which is the subject of current paper.

In order to obtain electromagnetic wave generation, one has to inject non-equilibrium spin into the upper subband. There are several ways to do this [33]. The most suitable for ferromagnetic metals are based on the spin pumping effect [34–38] and on the injection of spin-polarized current [39–41]. The spin pumping effect is usually quite weak. Further, it is hard to control the magnitude of the spin current. On the other hand, injection of non-equilibrium spin by a spin-polarized electric current is realized in a simple system consisting of two ferromagnets divided by a nonmagnetic interlayer. The voltage is applied to this system which causes the electric current to flow from one ferromagnet (spin source) to the other (active region). The amount of injected spin may be varied widely by changing the applied voltage. Therefore we consider this mechanism of non-equilibrium spin injection.

The paper is organized as follows. In Section 2 we perform calculations of electron transition probabilities for the four mentioned mechanisms. The transition probabilities are estimated for realistic parameters and are compared to each other. In Section 3 we consider a simple model in which non-equilibrium spin is injected into the ferromagnet by a spin-polarized electric current through a tunnel barrier. Then estimates of the radiation power and threshold electric current are performed.

2. Electron transition probabilities

We describe the conduction electrons by the hamiltonian (1) which takes into account the exchange coupling in the s-d model approach. The magnetization \mathbf{M} may either be constant or depend on coordinates (see (8)). Different types of interactions additionally taken into account lead to different probabilities of electron transitions between spin subbands. While the Rashba or Zeeman coupling may be taken into account in perturbation theory, a non-collinear magnetic system has rather different spin subbands.

2.1. Uniform ferromagnet. Rashba and Zeeman coupling

In this subsection we consider two mechanisms that exist in a uniform $\mathbf{M} = e_z$. The wave functions have the form (2) with corresponding energy of electrons:

$$\varepsilon_\pm = \frac{\hbar^2 k^2}{2m_e} \pm J. \quad (9)$$

In order to calculate the probability of electron transitions between spin subbands, we use the Fermi golden rule [17]

$$W_{kk'}^\pm = \frac{2\pi}{\hbar} |H_{kk'}^\pm|^2 \frac{\Delta/\pi}{(\Delta\varepsilon - \hbar\omega)^2 + \Delta^2} \quad (10)$$

where spin flip processes due to reasons other than interaction with electromagnetic wave (e.g. scattering on magnetic impurities) are taken

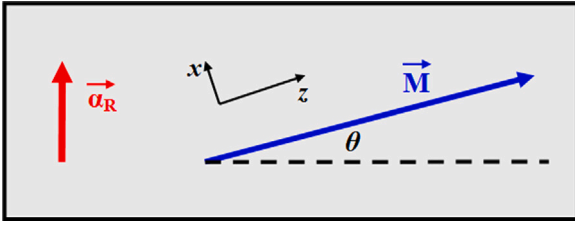


Fig. 1. Uniformly magnetized system with Rashba coupling. \mathbf{M} is directed along the z -axis; the angle between α_R and the x -axis is θ .

into account, $\tau_s = 2\pi\hbar/\Delta$ being the spin relaxation time; $H_{kk'}^\pm = \langle \psi_+ (\mathbf{k}') | \hat{H}^{int} | \psi_- (\mathbf{k}) \rangle$ is the matrix element of the hamiltonian of interaction of electrons with electromagnetic wave \hat{H}^{int} ; $(\mathbf{k}, -)$ and $(\mathbf{k}', +)$ are the initial and final states; $\Delta\varepsilon = \varepsilon_+ (\mathbf{k}') - \varepsilon_- (\mathbf{k})$ is the energy difference between these states.

Electron transitions due to the magnetic field of the wave are described by the interaction hamiltonian (5). The magnetization is assumed to be uniform. Using (10) we arrive at

$$W_Z^\pm = \frac{2}{\hbar} \left(\frac{e\hbar \|\mathbf{B} \times \mathbf{M}\|}{m_e c} \right)^2 \frac{\Delta}{(\Delta\varepsilon - \hbar\omega)^2 + \Delta^2} \delta(\mathbf{k} - \mathbf{k}'), \quad (11)$$

$\delta()$ is the Dirac delta-function. Only the magnetic field orthogonal to the magnetization \mathbf{M} participates in intersubband spin transitions. The momentum (or electron wave vector) is conserved here, as for all mechanisms of electron transitions considered below.

In order to find the probability of electron transitions due to Rashba spin-orbit coupling, it is necessary to take into account both (3) and (6). The coordinate system is chosen so that $\mathbf{M} = e_z$, and $\alpha_R = \alpha_R (e_x \cos\theta + e_z \sin\theta)$ (see Fig. 1) thus describing the general case. We restrict ourselves to the linear order in α_R . In this approximation the energy and wave functions are

$$\varepsilon_\pm = \frac{\hbar^2 k^2}{2m_e} \pm (J - \alpha_R k_y \cos\theta), \quad (12)$$

$$\psi_+ = \exp(i\mathbf{k}\mathbf{r}) \begin{pmatrix} 1 \\ -\frac{\alpha_R((k_y - ik_x)\sin\theta - ik_z \cos\theta)}{2J} \end{pmatrix}, \quad (13)$$

$$\psi_- = \exp(i\mathbf{k}\mathbf{r}) \begin{pmatrix} \frac{\alpha_R((k_y + ik_x)\sin\theta + ik_z \cos\theta)}{2J} \\ 1 \end{pmatrix}. \quad (14)$$

Substituting these wave functions into (10) with (3) as the interaction hamiltonian we see that the momentum is conserved and the matrix element of transitions is zero. Note that this property remains in higher orders in α_R . Thus there are no spin-flip electron transitions. However the Rashba hamiltonian (6) itself depends on the electron momentum. This momentum $\hat{\mathbf{p}} = -i\hbar\nabla$ should be shifted taking the account of \mathbf{A}_ω , as in other parts of the hamiltonian. In turn, this leads to the interaction hamiltonian written in (7). The hamiltonian (7) is linear in the Rashba interaction itself. Therefore its matrix elements should be found with the use of the wave functions (2). After substituting them into (10) we have

$$W_R^\pm = \frac{2}{\hbar} \left(\frac{e\alpha_R}{2\hbar\omega} \right)^2 (E_\tau^2 + E_y^2 \sin^2\theta) \frac{\Delta}{(\Delta\varepsilon - \hbar\omega)^2 + \Delta^2} \delta(\mathbf{k} - \mathbf{k}'), \quad (15)$$

where E_τ is the component of wave electric field which is orthogonal to α_R . It is obvious that in such an approach the electron transition probability is proportional to the square of the Rashba constant in the lowest order. The electrons transitions go most effectively when $\sin^2\theta = 1$, i.e. the Rashba vector α_R is either parallel or antiparallel to the magnetization \mathbf{M} . However it is of the same order for α_R perpendicular to \mathbf{M} .

2.2. Helical ferromagnet

In this subsection, we consider two mechanisms that exist due to the exchange interaction in a non-collinear magnetic state. The mechanism that follows from the dependence of the exchange constant J on the electron momentum is described by the interaction hamiltonian (4). It is important that if the magnetization is uniform ($\mathbf{M} = e_z$) this hamiltonian contains only $\hat{\sigma}_z$ and therefore it does not flip spins. In the literature this mechanism was suggested and studied for a non-collinear system that consists of two layers uniformly magnetized in different directions [20,23]. We now study this mechanism for the helical magnetization distribution (8).

Exact solutions of the Schrodinger equation with the hamiltonian (1) are known from the literature [42,43]:

$$\psi_+ = \frac{1}{\sqrt{1+v^2}} e^{-i\frac{\varepsilon_+}{\hbar}t + i\mathbf{k}\mathbf{r}} \begin{pmatrix} v e^{-i\frac{q}{2}z} \\ e^{i\frac{q}{2}z} \end{pmatrix}, \quad (16)$$

$$\psi_- = \frac{1}{\sqrt{1+v^2}} e^{-i\frac{\varepsilon_-}{\hbar}t + i\mathbf{k}\mathbf{r}} \begin{pmatrix} e^{-i\frac{q}{2}z} \\ -v e^{i\frac{q}{2}z} \end{pmatrix}, \quad (17)$$

where q is the wave vector that is determined by the spiral step, as before, and the constant $v(k_z)$ is determined by

$$v = \frac{j}{k_z q + \sqrt{j^2 + k_z^2 q^2}} \equiv \frac{-k_z q + \sqrt{j^2 + k_z^2 q^2}}{j} \quad (18)$$

where we introduce the notation $j = \frac{2m_e}{\hbar^2} J$. The eigenstates (16), (17) correspond to energy defined as

$$\varepsilon_\pm = \frac{\hbar^2}{2m_e} \left(k^2 + \frac{q^2}{4} \pm \sqrt{j^2 + k_z^2 q^2} \right). \quad (19)$$

After calculating the matrix elements of the hamiltonian (4) on the wave functions (16), (17) we get the electron transitions probability

$$W_J^\pm = \frac{2}{\hbar} \left(\frac{e\hbar}{m_e \omega} \left(\mathbf{E} \cdot \frac{\hbar \mathbf{k}_z}{J} \frac{\partial J}{\partial \mathbf{p}} \right) \right)^2 q^2 \frac{J^2}{\Delta\varepsilon^2} \frac{\Delta}{(\Delta\varepsilon - \hbar\omega)^2 + \Delta^2} \delta(\mathbf{k} - \mathbf{k}'). \quad (20)$$

This probability is proportional to $(ql_\omega)^2$ where $l_\omega \propto E$ is the magnitude of the classical oscillations of electrons in the wave electric field in the direction for which J depends on \mathbf{k} . Importantly, the smaller scale of the magnetization change leads to the larger effect. This is due to the fact that the effect is caused by the inhomogeneous non-collinear distribution of magnetization. It is also important to note that the electron energy change $\Delta\varepsilon$ depends on k_z for magnetic helicoid. Therefore the spin relaxation processes that lead to energy uncertainty are important here.

A mechanism that is solely due to the exchange coupling exists in non-collinear ferromagnets due to the minimal coupling described by (3). It does not need the dependence of the exchange constant J on the electron quasimomentum. The electron transitions probability determined by (10) for the interaction hamiltonian (3) with the wave functions (16), (17) is

$$W_{mc}^\pm = \frac{2}{\hbar} \left(\frac{e\hbar E_z}{2m_e \omega} \right)^2 q^2 \frac{J^2}{\Delta\varepsilon^2} \frac{\Delta}{(\Delta\varepsilon - \hbar\omega)^2 + \Delta^2} \delta(\mathbf{k} - \mathbf{k}'). \quad (21)$$

This probability is also proportional to $(ql_\omega)^2$, but the magnitude of the classical oscillations along the direction of the magnetization change are important here. Thus, (20) and (21) lead to different polarization properties.

2.3. Comparison of transition probabilities

In this subsection we compare all four obtained electron transition probabilities (11), (15), (20), and (21). The realistic parameters of both uniform and helical ferromagnets and boundaries are taken for our estimates. The probability W_{mc}^{\pm} obtained for a magnetic spiral is taken as a reference since it is solely due to the exchange coupling.

If we take $\hbar\omega \approx 2J$ thus supposing the resonant character of electron transitions then the ratio W_Z^{\pm}/W_{mc}^{\pm} may be roughly determined as $W_Z^{\pm}/W_{mc}^{\pm} \approx \left(\frac{4k_{\omega}}{q}\right)^2$, where $k_{\omega} = \frac{\omega}{c}$ is the wave vector of the electromagnetic wave in vacuum. Taking the parameters of holmium [30] $q \approx 10^7 \text{ cm}^{-1}$ (which corresponds to the spiral step 3.5 nm), $J \approx 0.185 \text{ eV}$ we obtain the estimation $W_Z^{\pm}/W_{mc}^{\pm} \approx 5.6 \cdot 10^{-5}$. For another example of a helical ferromagnet, manganese silicene, q is approximately 6 times smaller, and therefore $W_Z^{\pm}/W_{mc}^{\pm} \approx 1.8 \cdot 10^{-3}$. Thus, the magnetic dipole electron transitions due to the Zeeman term have very low probability and usually may be neglected. The transition probabilities depend on wave frequency in different ways, but the resonance should be shifted to very high frequency in order to obtain W_Z^{\pm} comparable to other transition probabilities. This does not correspond to any real system parameters. We therefore omit transitions due to the magnetic field of the wave below.

Comparing the Rashba mechanism to the exchange mechanism in helicoidal magnets, again for $\hbar\omega \approx 2J$, gives $W_R^{\pm}/W_{mc}^{\pm} \approx \left(\frac{m_e \alpha_R}{\hbar^2 q}\right)^2$. The Rashba interaction usually appears at interfaces. The value of α_R for ferromagnets may be estimated from the known value of the Dzyaloshinskii–Moriya interaction (DMI) that appears at the interfaces between transition ferromagnetic metals and heavy metals. The DMI constant was measured by the Brillouin light spectroscopy in a [Co/Pt] multilayer [44]. We use it to roughly estimate $\alpha_R \approx 1 \text{ peV m}$ which may be considered as an effective Rashba coupling averaged over the volume of the multilayer system. Then $W_R^{\pm}/W_{mc}^{\pm} \approx 0.013$ for holmium and ≈ 0.4 for MnSi. Therefore the Rashba interaction mechanism should be important even for simple ferromagnet interfaces. If we consider a three-layer system in which an interface on two non-magnetic materials with strong Rashba coupling is placed close to the ferromagnet then the Rashba coupling may become the main mechanism of the electron transitions between spin subbands. For example, $\alpha_R \approx 305 \text{ peV m}$ at a Bi/Ag interface [36]. So in a ferromagnet/Bi / Ag system with a thin Bi layer $W_R^{\pm}/W_{mc}^{\pm} \approx 4$ if holmium is taken to calculate W_{mc}^{\pm} and even larger in manganese silicene.

Two mechanisms of interband electron transitions in non-collinear ferromagnets defined by (20) and (21) have different symmetry with respect to the wave polarization: the first one is determined by the dependence of J on k and therefore by the crystallographic structure of the ferromagnet, while the second one is determined by the direction of magnetization change. The direction of change of magnetic moment in natural non-collinear ferromagnets such as holmium is strictly connected to their crystallographic directions and therefore these two mechanisms are similar in such natural ferromagnets. However in artificial ferromagnets the situation may change. In principle, in a polycrystalline magnetic structure with random directions of crystallographic axes the mechanism defined by (20) may vanish while (21) depends only on the magnetic structure and therefore may exist. In order to compare these two mechanisms quantitatively, we use the estimation from literature [20,21]

$$\left| \frac{\partial J}{\partial p} \right| \approx \frac{J}{p_0}, \quad (22)$$

where $p_0 = \frac{\hbar}{a}$, and $a \approx 10^{-8} \text{ cm}$ is the lattice constant. Then the ratio $W_J^{\pm}/W_{mc}^{\pm} \approx (k_z a)^2$. For $k_z \approx k_f$ and the Fermi energy $\epsilon_f = \frac{\hbar^2 k_f^2}{2m_e} \approx 5 \text{ eV}$ we have $W_J^{\pm}/W_{mc}^{\pm} \approx 1$. However the estimation (22) is very optimistic, and moreover 1 is obtained for the maximum value of k_z^2 . Therefore it seems that the electron transitions in a non-collinear ferromagnet that occur for constant J would be more effective than that which

appear from the dependence of J on the electron quasimomentum. Both mechanisms are of the same order of value and therefore should be taken into account simultaneously.

The obtained results are summed in the list below.

- i The probability of electron transitions between the spin subbands due to the Zeeman term is three to five orders smaller than that provided by the minimal coupling in typical ferromagnets with helical magnetization distribution such as holmium or manganese silicene. Therefore it can be neglected.
- ii The electron transition probability due to the Rashba coupling at the boundary of a ferromagnet and a heavy metal (such as Pt) is one or two orders smaller compared to that provided by the minimal coupling in the helical ferromagnets mentioned below. However it can be sufficiently increased if a system such as ferromagnet/Bi / Ag with a thin Bi interlayer (thickness is smaller than the spin relaxation length) is taken. In such a system, the Rashba coupling is obtained at an interface between bismuth and silver.
- iii Both the minimal coupling and the dependence of the exchange constant J on the electron momentum provide spin-flip electron transitions only in non-collinear ferromagnets. In typical helical ferromagnets (Ho or MnSi) they lead to the electron transition probabilities that are of the same order of value. Both these probabilities are inversely proportional to the characteristic scale of the magnetization change (the spiral period for helical magnetization distribution).

From this list, one may conclude that the minimal coupling and the dependence of the exchange constant J on the electron momentum are the most reliable mechanisms of the electromagnetic wave generation due to the spin-flip transitions of electrons. We further study the wave emission properties for these two mechanisms in a ferromagnet with helical magnetization distribution.

3. Emission rate and electromagnetic wave radiation power

The electron transition probabilities generally depend on the initial and final electron quasimomentum. In order to quantitatively determine the effectiveness of electron transitions we need to average them over the electron states. In order to obtain emission of the electromagnetic wave, one should provide a non-equilibrium electron distribution within the spin subbands. Therefore we consider a simple model of spin injection into the ferromagnet by a spin-polarized electric current. The power of electromagnetic wave radiation is also estimated.

The electromagnetic wave radiation power may be found knowing the stimulated emission rate R_{st} which is defined as

$$R_{st} = \int dk dk' W_{kk'}^{\pm} (f_+(k') - f_-(k)), \quad (23)$$

where f_{\pm} are the electron distribution functions in two subbands. This emission rate is an average characteristic of electron transitions. It is proportional to the intensity of electromagnetic wave, or the density of photons N_p :

$$R_{st} = G N_p, \quad (24)$$

where G depends on the electron distribution functions in two spin subbands. These distribution functions are non-equilibrium and are determined by the model of non-equilibrium spin injection into the system. Therefore we first consider a simple model of injection of spin into the ferromagnet and then study the emission properties in this system.

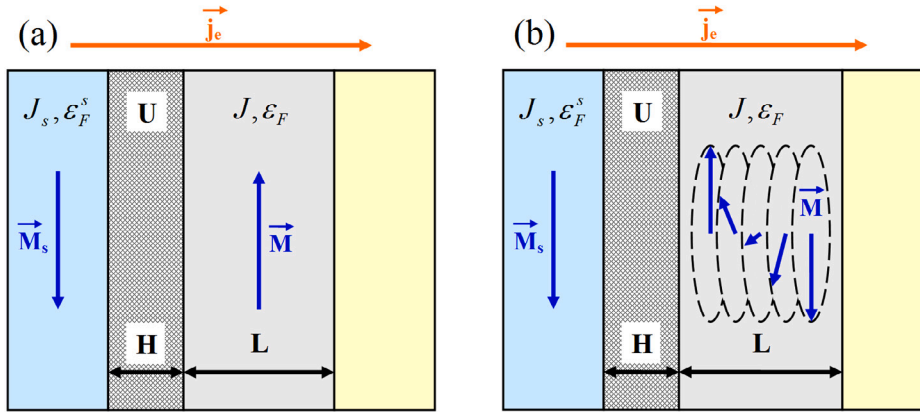


Fig. 2. Spin injection into a ferromagnet (active region with $\mathbf{M}, J, \epsilon_F$) from another ferromagnet (spin source with $\mathbf{M}_s, J_s, \epsilon_F^s$) for (a) uniform and (b) helicoidal active region.

3.1. Spin injection into a ferromagnet

We suppose that the electrons are injected into the ferromagnet (active region) from another ferromagnet by electric current through a tunnel barrier with constant height U and thickness H (see Fig. 2). The Fermi level in the ferromagnet that acts as a spin source ϵ_F^s is supposed to be greater than that in another ferromagnet ϵ_F which is the active region. In equilibrium, electrons tunnel from the spin source into the active region which leads to electric polarization of boundaries alike the contact potential difference. These tunneling processes are not important in the framework of the current paper and therefore are not considered. We suppose that the voltage V is applied to the system. This potential difference drops across the tunnel barrier. The probability of electron tunneling through the barrier that is linear in V is determined by the equation

$$P_{\pm}^{tunn} = A(U) (\epsilon - \epsilon_{\pm} \pm J_s), \quad (25)$$

where J_s is the exchange constant in the spin source, $A(U)$ is given by

$$A(U) = 2H \sqrt{\frac{2m_e}{\hbar^2}} \frac{eV}{U^2} \exp\left(-2H \sqrt{\frac{2m_e}{\hbar^2}} U\right), \quad (26)$$

and we assume that the barrier height U is much greater than the Fermi energy ϵ_F^s and the energy eVH gained by the electron in the electric field created by the voltage. The quantum number k in the direction along the normal to boundaries is mixed with the electron spin. Therefore we use quantum numbers ϵ which is the electron energy and $\epsilon_{\perp} = \frac{\hbar^2 k_{\perp}^2}{2m_e}$ where k_{\perp} is the quasimomentum along the surface of the boundaries (the direction of this quasimomentum is not important and therefore a simple integration over it leads to multiplication by 2π).

We suppose that the spin quantization axis is chosen as in the active region. The spin source magnetization has the direction opposite to the magnetization in the active region (see Fig. 2a), so that more electrons are injected into the upper spin subband than into the lower one. For the helicoidal magnetization the system is chosen so that the axis of the helix is perpendicular to the tunnel barrier surface. The magnetization of the spin source is directed oppositely to the magnetization of the active region at the boundary (Fig. 2b). In this case the electrons injected with spin parallel or antiparallel to the magnetization of the spin source may be roughly considered as injected into the corresponding minority or majority spin subband which may lead to the population inversion [33]. The probability (25) depends on the spin of the electron. It is non-zero for the energy of electron $\epsilon_F < \epsilon < \epsilon_F^s$ because all states with $\epsilon < \epsilon_F$ are occupied by other electrons in the active region and therefore tunneling to these states is impossible. On the other hand, $\epsilon < \epsilon_F^s$ is governed by the fact that there are no electrons with energy greater than ϵ_F^s in the spin source. The

range for ϵ_{\perp} is determined by the demand of real k along the normal to boundary surface. For the lower subband (“-”) $0 < \epsilon_{\perp} < \epsilon - J_s$ which is determined by the spin source. For the upper subband (“+”) $0 < \epsilon_{\perp} < \epsilon - J$ which is determined by the demand of real k in the active region. Note that there are electrons with $\epsilon - J < \epsilon_{\perp} < \epsilon + J_s$ in the spin source but they are reflected from the boundary.

The spin-polarized electric current is determined by the electron momentum averaged with the tunneling probability (25). After a simple calculation we arrive at

$$j_{e\pm} = A(U) \frac{\pi e m_e}{3\hbar^3} \left((\epsilon_F^s)^3 - \epsilon_F^3 \right) \left(1 \pm \frac{3}{2} \frac{\epsilon_F^s + \epsilon_F}{(\epsilon_F^s)^2 + \epsilon_F^2 + \epsilon_F \epsilon_F^s} (J_s - J) \right). \quad (27)$$

Taking into account that $j_{e+} + j_{e-} = j_e$ we find the constant $A(U)$ as

$$A(U) = j_e \frac{3\hbar^3}{2\pi e m_e \left((\epsilon_F^s)^3 - \epsilon_F^3 \right)}. \quad (28)$$

Eq. (28) together with (25) determines the tunneling probability via the electric current density j_e .

The electron density in the two spin subbands in the active region is denoted by N_{\pm} and the correction to this density due to spin polarized current by δN_{\pm} . We suppose that the total electron number does not change in time in the active region, i.e. the electrons are injected via the tunnel barrier and leave on the other side of the active region. In this case $\delta N_{\pm} = \delta N_0 \pm \delta N$, where the total number of injected electrons $2\delta N_0$ is constant and δN determines the electron spin polarization. In addition, we describe the system by the electron density averaged over the thickness of the active region. However we take into account spin relaxation within the active region. If the spin relaxation length is λ_s and the fraction of electrons injected into the upper (lower) spin subband with respect to the total number of injected electrons is $a_{\pm} = \frac{j_{e\pm}}{j_e}$ then the fraction of the electrons that leave the active region with the same spin is $\left(a_{\pm} - \frac{1}{2}\right) \exp\left(-\frac{L}{\lambda_s}\right) + \frac{1}{2}$ where L is the thickness of active region. We then have for the electron density averaged over the active region thickness

$$\delta \dot{N}_{+} = -\delta \dot{N}_{-} = \delta \dot{N} = \frac{j_e}{eL} \eta \left(1 - \exp\left(-\frac{L}{\lambda_s}\right) \right) - \frac{\delta N}{\tau_s}, \quad (29)$$

where τ_s is the spin relaxation time as before, and the efficiency of spin injection η is determined as

$$\eta = \frac{1}{2} \frac{j_{+} - j_{-}}{j_{+} + j_{-}} = \frac{3}{4} \frac{\epsilon_F^s + \epsilon_F}{(\epsilon_F^s)^2 + \epsilon_F^2 + \epsilon_F \epsilon_F^s} (J_s - J). \quad (30)$$

This corresponds to previously used equation for spin-polarized electron density [20,21,29] where η was introduced phenomenologically. It should be noted that the spin injection efficiency is determined by

both the exchange constant of spin source J_s and the exchange constant of active region J . If $J > J_s$ then there is no population inversion, i.e. more electrons are injected into lower spin subband than into upper one. In order to have $\eta > 0$ one needs to inject spins from a stronger ferromagnet than that is used as the active region, for which the inequality $J_s > J$ is satisfied. Eq. (29) determines the stationary non-equilibrium state with no stimulated emission:

$$\delta N^* = \frac{j_e \tau_s}{eL} \eta \left(1 - \exp\left(-\frac{L}{\lambda_s}\right) \right). \quad (31)$$

In this state the injected non-equilibrium spin is compensated by the spin relaxation process in the active region.

In the existing literature [20,21,23,29] it is implied that all injected electrons immediately relax to the lowest vacant states inside the spin subband, thus supposing that the energy relaxation time $\tau_e \ll \tau_s$, and in addition that $\tau_e \ll \frac{L}{v_F}$. However the typical time for an electron to pass through the active region $\frac{L}{v_F}$ is much smaller than τ_e for the thickness of the active region $L \sim 10$ nm (the electromagnetic wave emission is accompanied by a change of electron energy but these processes are supposed to give a small correction to τ_e) [45]. Therefore in the present work we assume that the electron energy does not relax within the active region (i.e. the electron transitions with photon emission are supposed to give a small correction to the distribution function which is beyond the scope of our consideration). The non-equilibrium correction to the electron distribution function is determined by the probability of electron injection (25):

$$\delta f_+ = j_e \frac{3\hbar^3 (\varepsilon - \varepsilon_\perp + J_s)}{4\pi m_e ((\varepsilon_F^s)^3 - \varepsilon_F^3)} \frac{\lambda_s}{L} \left(1 - e^{-\frac{L}{\lambda_s}} \right),$$

$$\varepsilon \in (\varepsilon_F, \varepsilon_F^s), \varepsilon_\perp \in (0, \varepsilon - J), \quad (32)$$

$$\delta f_- = j_e \frac{3\hbar^3 (\varepsilon - \varepsilon_\perp - J_s)}{4\pi m_e ((\varepsilon_F^s)^3 - \varepsilon_F^3)} \frac{\lambda_s}{L} \left(1 - e^{-\frac{L}{\lambda_s}} \right),$$

$$\varepsilon \in (\varepsilon_F, \varepsilon_F^s), \varepsilon_\perp \in (0, \varepsilon - J_s), \quad (33)$$

where we take into account the spin relaxation processes and average the distribution function over the thickness of the active region and also take into account that only electrons with positive k from the spin source to the active region contribute to δf_\pm . Note that the equilibrium electron distribution function is determined as

$$f_{0\pm} = 2, \varepsilon \in (\pm J, \varepsilon_F), \varepsilon_\perp \in (\pm, \varepsilon \mp J), \quad (34)$$

where we take into account that there are electrons with two signs of k_z for each energy level, and the nonequilibrium distribution function is $f_\pm = f_{0\pm} + \delta f_\pm$. It is important to note that the emission rate (23) contains the difference of electron densities at different energy rates $f_+(\varepsilon + \Delta\varepsilon) - f_-(\varepsilon)$, where $\Delta\varepsilon$ is the energy difference between two spin subbands.

We see from (32), (33) that the model of spin injection into the active region is very important because it determines the non-equilibrium electron distribution function. In our model, the result is obtained for the non-equilibrium distribution function in terms of j_e and thus does not directly contain the barrier height U .

3.2. Emission rate and critical current

Knowing the electron distribution function (32), (33) and the probability of electron transition between two spin subbands we may find the stimulated emission rate with the use of (23). There are two contributions into R_{st} . The first one ($R_{st}^{(1)}$) is due to the equilibrium part of the distribution function. Electrons with $\varepsilon \in (\varepsilon_F - 2J, \varepsilon_F)$ may transfer from the lower spin subband into the upper one because states with the same momentum have $\varepsilon > \varepsilon_F$ in the upper subband and therefore are free. Obviously, this makes a negative contribution to

R_{st} which corresponds to electromagnetic wave absorption. The second part ($R_{st}^{(2)}$) is due to the non-equilibrium correction to the distribution function. It may be positive for certain parameters, as it is shown below.

The energy difference between the two spin subbands $\Delta\varepsilon$ is constant and equal to $2J$ for uniform magnetization \mathbf{M} . For the magnetic helicoid the energy gap between spin subbands

$$\Delta\varepsilon = \frac{\hbar^2}{m_e} \sqrt{j^2 + k_z^2 q^2} \quad (35)$$

and thus depends on k_z . This dependence of $\Delta\varepsilon$ should be taken into account for $k_z \sim k_F$. For holmium, $q \sim 1.8 \cdot 10^7$ cm⁻¹ and $J \approx 0.185$ eV [2,30,32] which gives $j \sim 0.48 \cdot 10^{15}$ cm⁻², and taking $\varepsilon_F \approx 1$ eV we have $k_F q \sim 0.95 \cdot 10^{15}$ cm⁻². However the approximation $\Delta\varepsilon \approx 2J$ is sometimes useful because it allows us to integrate everything exactly. Moreover, it is correct for the mechanism due to the Rashba coupling in a uniform ferromagnet. Therefore we use this approximation first and then discuss the result and make corrections.

In order to find $R_{st}^{(1)}$ in this approximation one should substitute the equilibrium distribution function (34) and appropriate electron transition probability (15),(21),(20) into (23). Restricting ourselves to the lowest nonzero order in $\frac{J}{\varepsilon_F}$ and $\frac{J_s}{\varepsilon_F}$, we obtain after some calculations

$$R_{stR}^{(1)} = - \left(\frac{e [\alpha_R \times E]}{\hbar\omega} \right)^2 \frac{2\pi (2m_e)^{3/2}}{\hbar^4} \frac{\Delta}{(\hbar\omega - 2J)^2 + \Delta^2} \frac{J}{\varepsilon_F} \varepsilon_F^{3/2}, \quad (36)$$

$$R_{stmc}^{(1)} = - \left(\frac{e E_z}{\hbar\omega} \right)^2 \frac{2\pi q^2}{\sqrt{2m_e}} \frac{\Delta}{(\hbar\omega - 2J)^2 + \Delta^2} \frac{J}{\varepsilon_F} \varepsilon_F^{3/2}, \quad (37)$$

$$R_{stJ}^{(1)} = - \left(\frac{e \left(E \cdot \frac{\hbar k_F}{J} \frac{\partial J}{\partial p} \right)}{\hbar\omega} \right)^2 \frac{8\pi q^2}{3\sqrt{2m_e}} \frac{\Delta}{(\hbar\omega - 2J)^2 + \Delta^2} \frac{J}{\varepsilon_F} \varepsilon_F^{3/2}, \quad (38)$$

where we suppose that the Rashba vector is perpendicular to \mathbf{M} as shown in Fig. 2a (the Rashba vector is assumed to be perpendicular to the surface of the ferromagnet). The part of R_{st} determined by (36)–(38) depends only on the parameters of the active region. It does not depend on the electric current j_e . This is obvious since it corresponds to absorption of light by equilibrium electrons. In previous papers this part was not taken into account directly. However we show below that it is very important.

The contribution into R_{st} which appears due to non-equilibrium spin injection ($R_{st}^{(2)}$) is determined by $(\delta f_+(\varepsilon + \Delta\varepsilon) - \delta f_-(\varepsilon))$. It consists of two terms: one appears due to electron transitions from the upper subband into the lower one and is positive; the other appears due to backward electron transitions close to ε_F^s where $\delta f_+(\varepsilon + \Delta\varepsilon) = 0$ and is negative. Substituting the electron transition probabilities (15),(21),(20) and the non-equilibrium distribution functions (32), (33) into (23) and performing a simple calculation (with the use of the approximation $\Delta\varepsilon \approx 2J$) we arrive at

$$R_{stR}^{(2)} = \left(\frac{e [\alpha_R \times E]}{\hbar\omega} \right)^2 2\sqrt{\frac{2m_e}{\hbar^2}} \frac{\Delta \frac{\lambda_s}{L} \left(1 - e^{-\frac{L}{\lambda_s}} \right)}{(\hbar\omega - 2J)^2 + \Delta^2} \frac{J_s}{(\varepsilon_F^s)^{3/2}} \frac{j_e}{e}, \quad (39)$$

$$R_{stmc}^{(2)} = \left(\frac{e \hbar E_z}{2m_e \omega} \right)^2 2\sqrt{\frac{2m_e}{\hbar^2}} \frac{\Delta \frac{\lambda_s}{L} \left(1 - e^{-\frac{L}{\lambda_s}} \right)}{(\hbar\omega - 2J)^2 + \Delta^2} \frac{J_s}{(\varepsilon_F^s)^{3/2}} \frac{j_e}{e}, \quad (40)$$

$$R_{stJ}^{(2)} = \left(\frac{e \hbar \left(E \cdot \frac{\hbar k_F}{J} \frac{\partial J}{\partial p} \right)}{m_e \omega} \right)^2 \frac{2}{5} \sqrt{\frac{2m_e}{\hbar^2}} \frac{\Delta \frac{\lambda_s}{L} \left(1 - e^{-\frac{L}{\lambda_s}} \right)}{(\hbar\omega - 2J)^2 + \Delta^2} \frac{J_s}{(\varepsilon_F^s)^{1/2}} \frac{j_e}{\varepsilon_F}, \quad (41)$$

where we take $\varepsilon_F^s \gg \varepsilon_F$ and $J_s \gg J$ for simplicity. The result (39)–(41) depends both on the parameters of active region and spin source. Moreover, it is proportional to the electric current j_e . The total R_{st} is defined as $R_{st} = R_{st}^{(1)} + R_{st}^{(2)}$. Since $R_{st}^{(1)}$ depends only on the parameters of

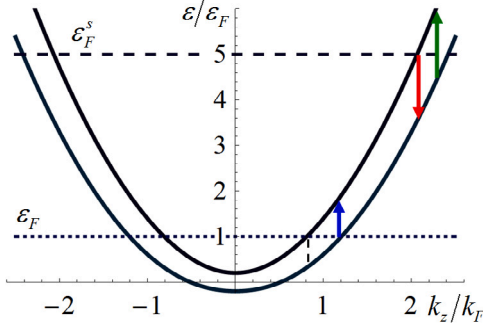


Fig. 3. Spin subbands in a helicoidal ferromagnet for $\varepsilon_F^s = 5\varepsilon_F$, $\frac{J}{\varepsilon_F} = 0.2$, $\frac{q}{k_F} = 0.34$. Three arrows have different length which corresponds to different $\Delta\varepsilon$.

active region it is possible to obtain positive R_{st} by taking appropriate spin source and current.

It is obvious that for small current R_{st} is negative. The critical electric current j_e^c is defined as the current at which R_{st} becomes positive, i.e. $R_{st}^{(2)}(j_e^c) = R_{st}^{(1)}$, and the wave absorption is exactly compensated by emission at j_e^c . If $\varepsilon_F^s \gg \varepsilon_F$ Eqs. (39)–(41) are simplified. Equating (39)–(41) to the corresponding (36)–(38) we find the critical electric current:

$$j_{eR}^c = j_{emc}^c = \frac{\pi}{2} e k_F^3 \frac{\hbar k_F^s}{m_e} \frac{J/\varepsilon_F}{J_s/\varepsilon_F^s} \frac{L/\lambda_s}{1 - e^{-L/\lambda_s}}, \quad (42)$$

$$j_{eJ}^c = \frac{10\pi}{3} e k_F^3 \frac{\hbar k_F^s}{m_e} \left(\frac{k_F}{k_F^s}\right)^2 \frac{J/\varepsilon_F}{J_s/\varepsilon_F^s} \frac{L/\lambda_s}{1 - e^{-L/\lambda_s}}. \quad (43)$$

One can see that the obtained electric current is extremely high for any reasonable system parameters (for example, if we take $\varepsilon_F \sim 1$ eV, $\varepsilon_F^s \sim 5$ eV, $\frac{J}{\varepsilon_F} \sim \frac{J_s}{\varepsilon_F^s} \sim 0.2$ and $L \ll \lambda_s$, we obtain $5 \cdot 10^{12} \frac{A}{cm^2}$ from (42) and $3 \cdot 10^{12} \frac{A}{cm^2}$ from (43)).

The physical meaning of this result is following. There are more electrons in the lower spin subband of the active region than in the upper one. These electrons may transit into the upper subband under the influence of electromagnetic wave if there are free states in the upper subband corresponding to the same electron momentum. This leads to the electromagnetic wave absorption which was discussed for noncollinear magnetic systems in [32] and is not taken into account directly in papers devoted to electromagnetic wave generation due to transitions between spin subbands in ferromagnet. Roughly, it is needed to inject more electrons into the upper spin subsystem than the excess in the lower one in order to obtain generation of electromagnetic wave. This excess of the electrons is rather big ($\sim N_e \frac{J}{\varepsilon_F} \sim 0.2N_e$ where N_e is the total electron concentration in the active region). When calculating the emission rate, the electron concentration is multiplied by a weight, i.e. the electron transition probability, which gives (42), (43).

One possible way to overcome this problem is to use a non-metal ferromagnet such as a magnetic semiconductor as an active region. We do not consider such possibility hereafter. Thus, in our consideration the mechanism of electromagnetic wave generation induced by Rashba coupling needs a very big electric current and therefore is not realistic.

Another way that works for non-collinear ferromagnet is to take into account that $\Delta\varepsilon$ depends on the quasimomentum k_z (z is the helicoid axis, see (8)). Indeed, the electrons that participate in electromagnetic wave absorption are mostly concentrated close to the Fermi sphere $\varepsilon \approx \varepsilon_F$ of the active region. On the other hand, the electrons that are injected from the spin source have the energy up to the Fermi energy of spin source ε_F^s . Therefore they may emit electromagnetic wave with different frequency when transit between spin subbands than that is absorbed well (see Figure 3). Thus, the critical current depends on frequency of electromagnetic wave. For relatively weak spin relaxation

processes (small Δ) this current may be small enough to be realized in experiment.

The exact result that is represented in the form of several integrals may be found in Appendix. Fig. 4 contains the results of numerical calculations of the critical current with respect to dimensionless wave frequency $\theta = \frac{\hbar\omega}{2J}$ and dimensionless spin relaxation parameter $\delta = \frac{\Delta}{2J}$. Other parameters are taken as before: $\varepsilon_F = 1$ eV, $\varepsilon_F^s = 5$ eV, $\frac{J}{\varepsilon_F} = \frac{J_s}{\varepsilon_F^s} = 0.2$, $q = 1.8 \cdot 10^7$ cm⁻¹. The spin relaxation length $\lambda_s = 20$ nm which is typical for ferromagnetic metals [46,47], and we take thickness of the active region $L = 5$ nm. The dependence of j_{emc}^c and j_{eJ}^c on frequency is shown in Figure 4a and b, correspondingly, for three different values of δ . It is plotted for $\hbar\omega > 2J$ because for smaller frequency the critical current is very big, which corresponds to our estimations (42), (43). When the frequency increases (starting at $2J$) the critical current decreases because the wave absorption by equilibrium electrons (the leftmost (blue) arrow in Fig. 3) becomes weaker while the wave emission by the injected non-equilibrium electrons is stronger (the middle (red) arrow in Fig. 3). The wave absorption by electrons which are injected into lower subband starts approximately at the steep decrease of j_e^c . This leads to growth of the critical current with further increase of the frequency, and finally there is a frequency interval in which R_{st} is negative for any current. This interval corresponds to high k_z at which only electrons injected into lower spin subband exist (the rightmost (green) arrow in Fig. 3). Contrary to the absorption of electromagnetic wave by the equilibrium electrons, the absorption of the wave by injected electrons depends on the electric current j_e and therefore makes stimulated emission impossible for any electric current in the corresponding frequency interval. At high frequencies, R_{st} becomes positive, but only for a very large current.

The critical current dependence on δ for both mechanisms is plotted in Fig. 4c for $\frac{\hbar\omega}{2J} = 3$ which is close to the minimum of j_e^c . We see that the critical current decreases linearly and is as small as $10^5 \frac{A}{cm^2}$ for $\delta = 10^{-8}$ which corresponds to spin relaxation time $\tau_s \sim 10^{-6}$ s. Although it is hard to imagine such small spin relaxation time, it seems possible to achieve critical current in pulse mode for very clean ferromagnet with $\tau_s \sim 10^{-9} - 10^{-10}$ s.

3.3. Radiation power

Here we perform a simple estimate of the power of stimulated emission of electromagnetic radiation in a helicoid due to two possible mechanisms of electron transitions between spin subbands. Our estimate of critical current and R_{st} in the previous subsection were performed for the stationary non-equilibrium state (31) that does not take into account the electromagnetic wave emission. For small deviations of δN from δN^* determined by (31) we may assume a linear dependence of R_{st} on δN (this is confirmed by the results of previous work for relatively small current [29]). Using Eq. (24) we may suppose $G(\delta N) = G(\delta N^*) \frac{\delta N}{\delta N^*}$. In order to simplify the calculation, we re-write this equation in terms of j_e^c as

$$G(\delta N) = \xi \frac{\delta N}{\delta N^*} (j_e - j_e^c), \quad (44)$$

where ξ does not depend on current. Note that we do not discuss the polarization properties of generated waves here, providing just simple estimations.

The equations for the photon density N_p and the non-equilibrium electron density δN are written as

$$\dot{N}_p = G(\delta N) N_p - \nu_p N_p, \quad (45)$$

$$\delta \dot{N} = \frac{j_e}{eL} \eta \left(1 - e^{-\frac{L}{\lambda_s}}\right) - \frac{\delta N}{\tau_s} - G(\delta N) N_p, \quad (46)$$

where Eq. (29) for δN is modified in order to take into account electron transitions with the emission of electromagnetic wave. Using Eq. (44) one can easily obtain a stationary state with nonzero photon density:

$$N_p^{**} = \frac{\delta N^* j_e - j_e^{th}}{\nu_p \tau_s j_e - j_e^c}, \quad (47)$$

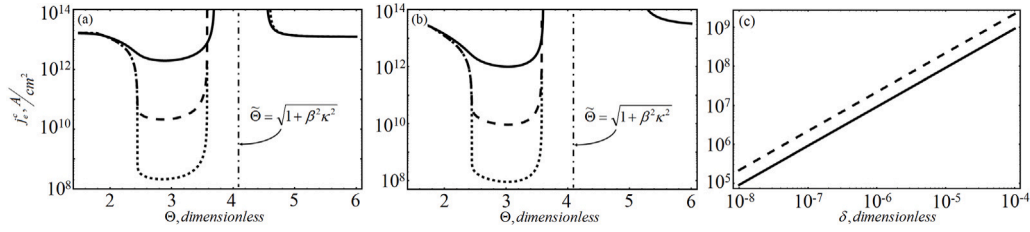


Fig. 4. Dependence of critical current (a) j_{emc}^c and (b) j_J^c on the dimensionless frequency $\Theta = \frac{\hbar\omega}{2J}$ for the spin relaxation parameter $\delta = \frac{\Lambda}{2J}$ equal to 10^{-1} (solid line), 10^{-3} (dashed line), and 10^{-5} (dotted line). The vertical dash-dotted lines correspond to $\tilde{\Theta} = \sqrt{1 + \beta^2 \kappa^2}$ which is determined by the maximal energy of the injected electrons. (c) Dependence of j_e^c (solid line) and j_{emc}^c (dashed line) on δ at frequency corresponding to $\Theta = 3$.

$$\delta N^{**} = \delta N^* \frac{v_p}{\xi (j_e - j_e^c)}, \quad (48)$$

where the threshold current is defined as

$$j_e^{th} = j_e^c + \frac{v_p \tau_s}{\xi}. \quad (49)$$

For the electric current $j_e < j_e^{th}$ there is no stationary state with nonzero photon density, while for $j_e > j_e^{th}$ such a stationary state exists and hence stimulated electromagnetic wave emission is possible. Obviously, the threshold current j_e^{th} is greater than the critical current j_e^c at which the wave emission exceeds the absorption. We have taken into account the electromagnetic wave emission by the medium in the form of $R_{st}^{(1)}$ which does not depend on the electric current. Here we suppose that the photon losses determined by v_p are due to the escape of photons from a resonator that contains the active region (i.e. v_p is the inverse photon lifetime in the resonator). Therefore the power of electromagnetic radiation emitted from the resonator may be estimated as

$$P_{rad} = \hbar\omega v_p N_p^{**} V_{res} = \hbar\omega \frac{\eta j_e}{eL} \left(1 - e^{-\frac{L}{\lambda_s}}\right) \frac{j_e - j_e^{th}}{j_e - j_e^c} V_{res}, \quad (50)$$

where V_{res} is the resonator volume. It is seen from (49) and (50) that the increase of v_p leads to growth of j_e^{th} while P_{rad} does not change. Therefore it is necessary to make a high quality resonator in order to obtain stimulated radiation.

In order to estimate the threshold current and radiation power, we take the same parameters as before. The frequency parameter is taken as $\Theta = 3$ which corresponds to the wavelength $\lambda = 1 \mu\text{m}$, the spin relaxation time $\tau_s \sim 10^9$. We estimate the resonator volume as $V_{res} \sim \lambda^3$. The inverse photon lifetime in the resonator is taken as $v_p \sim 3 \cdot 10^9 \text{ s}^{-1}$ which corresponds to the quality factor 10^5 if the resonator length is $\sim \lambda$. For these parameters the critical currents are $j_{emc}^c \approx 2.2 \cdot 10^8 \frac{\text{A}}{\text{cm}^2}$, $j_J^c \approx 9.2 \cdot 10^7 \frac{\text{A}}{\text{cm}^2}$, the threshold current is $j_e^{th} \approx 2.4 \cdot 10^8 \frac{\text{A}}{\text{cm}^2}$, $j_e^{th} \approx 9.9 \cdot 10^7 \frac{\text{A}}{\text{cm}^2}$. These currents may be achieved in pulse mode. The radiation power for $j_e = 3 \cdot 10^8 \frac{\text{A}}{\text{cm}^2}$ which is above the threshold for both mechanisms is $P_{rad}^{mc} \approx 78 \text{ W}$, $P_{rad}^{Jd} \approx 98 \text{ W}$ inside the pulse. The estimated power is rather large which is caused by high emission rate R_{st} in the considered system. Note that both mechanisms give similar values of threshold currents and radiation power. Therefore they should be taken into account simultaneously.

It should be noted here that our model does not take into account the radiation resistance. Hence very large power is obtained. This is much greater than the power of ohmic losses. In real experiment the increase of the radiation power would decrease current and lead the system to the boundary of generation region. This would keep the radiation power close to the power of ohmic losses by the order of value (several milliwatts). However this deserves a separate study and is beyond the scope of the present work.

4. Conclusion

We theoretically study possible mechanisms of the electromagnetic wave emission due to the transitions of conductance electrons between spin subbands in a ferromagnet. Four possible mechanisms are

considered. Two of them exist in a uniformly magnetized media: the Zeeman coupling to the magnetic field of the wave described by (5) and the Rashba spin-orbit coupling (6) which leads to the interaction hamiltonian (7) both lead to the mentioned electron transitions. A non-collinear magnetization distribution brings about two other mechanisms: one follows from the minimal coupling which leads to (3), the other is due to the dependence of the exchange constant J in the s-d exchange hamiltonian (1) on the electron momentum and is described by the interaction hamiltonian (4).

We compare the four mentioned mechanisms. We show that the mechanism of electron transitions caused by the magnetic field of the wave is much weaker than three other mechanisms, and therefore it could be neglected. The Rashba coupling taken for a simple boundary of a ferromagnet and a heavy metal such as Pt is shown to give a sufficiently smaller electron transition probability compared to two other mechanisms. However for a specially prepared boundary such as a ferromagnet/Bi/Ag system with a very thin (smaller than the spin relaxation length) Bi layer the electron transitions mediated by the Rashba coupling may be the dominant mechanism. The probabilities of the electron transitions due to the minimal coupling and the dependence of the exchange constant on the electron momentum in a non-collinearly magnetized medium are of the same order of value for realistic parameters. Both these probabilities are inversely proportional to the characteristic scale of the magnetization change (the spiral period for helical magnetization distribution). Therefore one should take the magnetic system with sharp magnetization change for the experiment (holmium is better than manganese silicene).

We consider a simple model of spin injection into a ferromagnet. We assume that the spin polarized electrons are injected by the electric current flowing from another ferromagnet with opposite magnetization direction through a tunneling barrier. (If a non-collinear ferromagnet is considered, the magnetization direction of the spin source is antiparallel to the magnetization of the non-collinear ferromagnet at the surface.) It is shown that the wave absorption in a uniform ferromagnet is very strong. This leads to an unrealizable critical electric current at which the emission rate becomes positive, i.e. the wave emission exceeds its absorption. The helical magnetization distribution brings about two main effects. The first one is additional mechanisms of the electromagnetic wave generation, as mentioned above. These mechanisms are due to the exchange coupling and therefore are the strongest among others. The second effect is the dependence of the energy gap (35) between spin subbands on the electron momentum. This diminishes the parasitic effect of the *intrinsic* electromagnetic wave absorption.

The threshold current (49) of the electromagnetic wave generation, in addition to the intrinsic wave absorption, takes into account all external wave losses in the system. We estimate this current for a non-collinear helicoidal magnetization distribution. We show that both the minimal coupling and the dependence of the exchange constant on the electron quasimomentum give similar estimates of the threshold current and radiation power. Such threshold current may be realized in an experiment. The corresponding frequency turns out to be approximately three times greater than the gap $2J$ between spin subbands at

zero electron momentum. However it follows from our calculations that the considered generation effect is very demanding on the parameters of the system. A very clean ferromagnet with the spin relaxation time $\tau_s \sim 10^{-9} - 10^{-10}$ s should be used in order to obtain a realizable critical current.

CRediT authorship contribution statement

E.A. Karashtin: Conceptualization, Methodology, Software, Formal analysis, Investigation, Writing.

Declaration of competing interest

The authors declare that they have no known competing financial interests or personal relationships that could have appeared to influence the work reported in this paper.

Funding

This work was supported by Center of Excellence ‘‘Center of Photonics’’ funded by The Ministry of Science and Higher Education of the Russian Federation, contract #075-15-2020-906.

Appendix. The exact expressions for the emission rate

Here we provide equations for the emission rates and critical current for two mechanisms of wave emission in non-collinear ferromagnet considered in current paper. These equations are exact with respect to $\frac{J}{\epsilon_F}$ and $\frac{J_s}{\epsilon_F^s}$. However the probability of electron tunneling through the barrier is the same as in the main body of the paper and is determined by (25) supposing that the potential barrier height $U \gg \epsilon_F, \epsilon_F^s$.

In order to describe numerous material parameters of the system, it is convenient to introduce dimensionless parameters $\kappa = \frac{k_F^s}{k_F} = \sqrt{\frac{\epsilon_F^s}{\epsilon_F}}$, $\chi = \frac{J_s}{J}$, $\beta = e \frac{qk_F}{j} (j = \frac{2m_e}{\hbar^2} J)$, $\delta = \frac{A}{2J}$, and $\Theta = \frac{\hbar\omega}{2J}$. Then $R_{st}^{(1)}$ and $R_{st}^{(2)}$ are re-written in exact form as

$$R_{st\ hel}^{(1)} = -\frac{\pi \hbar k_F^3}{(2J)^3} \left(\frac{e \hbar E_z q}{2m_e} \right)^2 I_{hel}^{(1)}(\Theta), \quad (A.1)$$

$$R_{st\ hel}^{(2)} = \frac{\pi \hbar k_F^3}{(2J)^3} \left(\frac{e \hbar E_z q}{2m_e} \right)^2 \frac{j_e}{e} \frac{3 \hbar^3}{4 \pi m_e \epsilon_F^2} \frac{\lambda_s}{L} \left(1 - e^{-\frac{L}{\lambda_s}} \right) \frac{1}{\kappa_s^6 - 1} I_{hel}^{(2)}(\Theta), \quad (A.2)$$

$$R_{st\ J}^{(1)} = -\frac{\pi \hbar k_F^3}{(2J)^3} \left(\frac{e \hbar q}{m_e} \left(\mathbf{E} \cdot \frac{\hbar k_F}{J} \frac{\partial J}{\partial \mathbf{p}} \right) \right)^2 I_J^{(1)}(\Theta), \quad (A.3)$$

$$R_{st\ J}^{(2)} = \frac{\pi \hbar k_F^3}{(2J)^3} \left(\frac{e \hbar q}{m_e} \left(\mathbf{E} \cdot \frac{\hbar k_F}{J} \frac{\partial J}{\partial \mathbf{p}} \right) \right)^2 \frac{j_e}{e} \frac{3 \hbar^3}{4 \pi m_e \epsilon_F^2} \times \frac{\lambda_s}{L} \left(1 - e^{-\frac{L}{\lambda_s}} \right) \frac{1}{\kappa_s^6 - 1} I_J^{(2)}(\Theta), \quad (A.4)$$

where the dimensionless frequency functions $I_{hel}^{(1,2)}(\Theta)$, $I_J^{(1,2)}(\Theta)$ are defined in the form of integrals:

$$I_{hel\ J}^{(1)}(\Theta) = \int_0^{x_-} dx F_{hel\ J}(x, \Theta) \left(1 - x^2 + \gamma \sqrt{1 + \beta^2 x^2} \right) - \int_0^{x_+} dx F_{hel\ J}(x, \Theta) \left(1 - x^2 - \gamma \sqrt{1 + \beta^2 x^2} \right), \quad (A.5)$$

$$I_{hel\ J}^{(2)}(\Theta) = \int_0^{x_+} dx F_{hel\ J}(x, \Theta) (\kappa^2 - 1) \left(x^2 + \gamma \left(\sqrt{1 + \beta^2 x^2} + \chi \right) \right) + \int_{x_+}^{x_-} dx F_{hel\ J}(x, \Theta) \left(\kappa^2 - x^2 - \gamma \sqrt{1 + \beta^2 x^2} \right)$$

$$\begin{aligned} & \times \left(x^2 + \gamma \left(\sqrt{1 + \beta^2 x^2} + \chi \right) \right) \\ & - \int_{\tilde{x}}^{x_-} dx F_{hel\ J}(x, \Theta) (\kappa^2 - \mu) \\ & \times \left(x^2 - \gamma \left(\sqrt{1 + \beta^2 x^2} + \chi \right) \right) \\ & - \int_{x_+}^{x_-} dx F_{hel\ J}(x, \Theta) \\ & \times \left(\kappa^2 - x^2 + \gamma \sqrt{1 + \beta^2 x^2} \right) \\ & \times \left(x^2 - \gamma \left(\sqrt{1 + \beta^2 x^2} + \chi \right) \right), \end{aligned} \quad (A.6)$$

$$F_{hel}(x, \Theta) = \frac{\delta}{\Theta^2 (1 + \beta^2 x^2) \left(\delta^2 + \left(\Theta - \sqrt{1 + \beta^2 x^2} \right)^2 \right)}, \quad (A.7)$$

$$F_J(x, \Theta) = x^2 F_{hel}(x, \Theta), \quad (A.8)$$

the constant μ in (A.6) is defined as $\mu = \max(1, \gamma \chi)$ depending on system parameters, and the dimensionless integration limits are the following:

$$x_{\pm} = \sqrt{1 + \frac{\beta^2 \gamma^2}{2} \mp \sqrt{1 + \beta^2 + \frac{\beta^4 \gamma^2}{4}}}, \quad (A.9)$$

$$x_{\pm}^s = \sqrt{\kappa^2 + \frac{\beta^2 \gamma^2}{2} \mp \sqrt{1 + \kappa^2 \beta^2 + \frac{\beta^4 \gamma^2}{4}}}, \quad (A.10)$$

$$\tilde{x} = \sqrt{\gamma \chi + \frac{\beta^2 \gamma^2}{2} + \gamma \sqrt{1 + \beta^2 \gamma \chi + \frac{\beta^4 \gamma^2}{4}}}, \quad (A.11)$$

$$x_-^a = \max(x_-, \tilde{x}). \quad (A.12)$$

Note that \tilde{x} stands for the smallest k_z at which the electrons are injected into the lower spin subband of the active region from the upper spin subband of the spin source (in the latter, there are no electrons with the energy corresponding to small k_z in the lower subband in the active region; k_z is not conserved at the boundary). The third integral in the right-hand part of (A.6) is zero if $\tilde{x} > x_-$. This condition depends on the system parameters in a complex way. But is exactly true if $\epsilon_F < J_s$ ($\gamma \chi > 1$ in dimensionless notation). In (A.6), we take into account both reduction of the electromagnetic wave absorption by equilibrium electrons due to the appearance of electrons in the upper spin subband lead by the electric current and absorption of electromagnetic wave by the electrons injected into lower spin subband which is stronger than emission due to the inverse process at high k_z for which there are no injected electrons in the upper spin subband.

Applying a condition of positive R_{st} leads us to the critical current $j_e^c(\theta)$

$$j_e^c(\theta) = e \frac{\pi}{3} k_F^3 \frac{\hbar k_F}{m_e} \frac{L/\lambda_s}{1 - e^{-\frac{L}{\lambda_s}}} (\kappa_s^6 - 1) \frac{I_{hel\ J}^{(1)}(\Theta)}{I_{hel\ J}^{(2)}(\Theta)}. \quad (A.13)$$

One can see that the exact Eq. (A.13) for the critical current contains dependence on the wave frequency which is very important if small parameter δ (that stands for the spin relaxation) is taken.

References

- [1] I.S. Grigoriev, E.Z. Meilikhov (Eds.), *The Handbook of Physical Quantities*, CRC Press, Boca Raton, FL, United States, 1996.
- [2] P. Weber, M. Dressel, *Effect of magnetic ordering on the infrared spectra of holmium*, 272–276, 2004, p. E1109.
- [3] O.G. Udalov, M.V. Sapozhnikov, E.A. Karashtin, B.A. Gribkov, S.A. Gusev, E.V. Skorohodov, V.V. Rogov, A.Y. Klimov, A.A. Fraerman, *Nonreciprocal light diffraction by a lattice of magnetic vortices*, Phys. Rev. B 86 (2012) 094416, <http://dx.doi.org/10.1103/PhysRevB.86.094416>, <https://link.aps.org/doi/10.1103/PhysRevB.86.094416>.

- [4] A.A. Fraerman, B.A. Gribkov, S.A. Gusev, A.Y. Klimov, V.L. Mironov, D.S. Nikitushkin, V.V. Rogov, S.N. Vdovichev, B. Hjorvarsson, H. Zabel, Magnetic force microscopy of helical states in multilayer nanomagnets, *J Appl Phys* 103 (7) (2008) 073916, <http://dx.doi.org/10.1063/1.2903136>.
- [5] E.S. Demidov, N.S. Gusev, L.I. Budarin, E.A. Karashtin, V.L. Mironov, A.A. Fraerman, Interlayer interaction in multilayer [Co/Pt]_n/Pt/Co structures, *J Appl Phys* 120 (17) (2016) 173901, <http://dx.doi.org/10.1063/1.4967163>.
- [6] V.L. Mironov, O.L. Ermolaeva, S.A. Gusev, A.Y. Klimov, V.V. Rogov, B.A. Gribkov, O.G. Udalov, A.A. Fraerman, R. Marsh, C. Checkley, R. Shaikhaidarov, V.T. Petrashev, Antivortex state in crosslike nanomagnets, *Phys. Rev. B* 81 (2010) 094436, <http://dx.doi.org/10.1103/PhysRevB.81.094436>, <https://link.aps.org/doi/10.1103/PhysRevB.81.094436>.
- [7] M.V. Sapozhnikov, L.I. Budarin, E.S. Demidov, Ferromagnetic resonance of 2D array of magnetic nanocaps, *J. Magn. Magn. Mater.* 449 (2018) 68–76, <http://dx.doi.org/10.1016/j.jmmm.2017.09.082>.
- [8] E.V. Skorokhodov, R.V. Gorev, M.V. Sapozhnikov, V.L. Mironov, Manifestation of ferromagnetic resonance of permalloy microstrips in magnetic force spectroscopy measurements, *J. Magn. Magn. Mater.* 491 (2019) <http://dx.doi.org/10.1016/j.jmmm.2019.165538>.
- [9] M.V. Sapozhnikov, N.S. Gusev, S.A. Gusev, D.A. Tatarskiy, Y.V. Petrov, A.G. Temiryazev, A.A. Fraerman, Direct observation of topological hall effect in Co/Pt nanostructured films, *Phys. Rev. B* 103 (2021) 054429, <http://dx.doi.org/10.1103/PhysRevB.103.054429>, <https://link.aps.org/doi/10.1103/PhysRevB.103.054429>.
- [10] T. Kampfrath, M. Battiato, P. Maldonado, G. Eilers, J. Notzold, S. Mahrlein, V. Zbarsky, F. Freimuth, Y. Mokrousov, S. Blugel, M. Wolf, I. Radu, P.M. Oppeneer, M. Munzenberg, *Nature Nanotechnology* 8 (2013) 256, <http://dx.doi.org/10.1038/NNANO.2013.43>.
- [11] T. Seifert, S. Jaiswal, U. Martens, J. Hannegan, L. Braun, P. Maldonado, F. Freimuth, A. Kronenberg, J. Henrzi, I. Radu, E. Beaupaire, Y. Mokrousov, P.M. Oppeneer, M. Jourdan, G. Jakob, D. Turchinovich, L.M. Hayden, M. Wolf, M. Munzenberg, M. Kläui, T. Kampfrath, *Nature Photonics* 10 (2016) 483, <http://dx.doi.org/10.1038/NPHOTON.2016.91>.
- [12] D.S. Bulgarevich, Y. Akamine, M. Talara, V. Mag-usara, H. Kitahara, H. Kato, M. Shihara, M. Tani, M. Watanabe, *Sci. Rep.* 10 (2020) 1158, <http://dx.doi.org/10.1038/s41598-020-58085-5>.
- [13] R. Adam, G. Chen, D.E. Bürgler, T. Shou, I. Komissarov, S. Heidtfeld, H. Hardtdegen, M. Mikulics, C.M. Schneider, R. Sobolewski, Magnetically and optically tunable terahertz radiation from Ta/NiFe/Pt spintronic nanolayers generated by femtosecond laser pulses, *Appl. Phys. Lett.* 114 (21) (2019) 212405, <http://dx.doi.org/10.1063/1.5099201>.
- [14] U. Nandi, M.S. Abdelaziz, S. Jaiswal, G. Jakob, O. Gueckstock, S.M. Rouzegar, T.S. Seifert, M. Kläui, T. Kampfrath, S. Preu, Antenna-coupled spintronic terahertz emitters driven by a 1550 nm femtosecond laser oscillator, *Appl. Phys. Lett.* 115 (2) (2019) 022405, <http://dx.doi.org/10.1063/1.5089421>.
- [15] A. Melnikov, I. Razdolski, T.O. Wehling, E.T. Papaioannou, V. Roddatis, P. Fumagalli, O. Aktsipetrov, A.I. Lichtenstein, U. Bovensiepen, Ultrafast transport of laser-excited spin-polarized carriers in Au/Fe/MgO(001), *Phys. Rev. Lett.* 107 (2011) 076601, <http://dx.doi.org/10.1103/PhysRevLett.107.076601>, <https://link.aps.org/doi/10.1103/PhysRevLett.107.076601>.
- [16] S.V. Vonsovskii, *Magnetism*, Wiley, New York, 1974.
- [17] L.D. Landau, E.M. Lifshitz, *Course of Theoretical Physics, Vol. 3: Quantum Mechanics (Non-Relativistic Theory)*, Butterworth - Heinemann, Oxford, 1991.
- [18] L.D. Landau, E.M. Lifshitz, *Course of Theoretical Physics, Vol. 8: Electrodynamics of Continuous Media*, Butterworth - Heinemann, Oxford, 1984.
- [19] G. Tatara, Effective gauge field theory of spintronics, *Physica E: Low-dimensional Syst. Nanostruct.* 106 (2019) 208–238, <http://dx.doi.org/10.1016/j.physe.2018.05.011>, <https://www.sciencedirect.com/science/article/pii/S1386947717318398>.
- [20] A. Kadigrobov, Z. Ivanov, T. Claeson, R.I. Shekhter, M. Jonson, *Europhys. Lett.* 67 (2004) 948.
- [21] A. Kadigrobov, R.I. Shekhter, M. Jonson, *Low Temp. Phys.* 31 (2005) 352.
- [22] N.A. Viglin, V.V. Ustinov, V.M. Tsvelikhovskaya, O.F. Denisov, *JETP Lett.* 84 (2006) 79.
- [23] Y.V. Gulyaev, E.A. Vilkov, P.E. Zil'berman, G.M. Mikhailov, S.G. Chigarev, *J. Commun. Technol. Electron.* 58 (2013) 1137.
- [24] R.I. Shekhter, A.M. Kadigrobov, M. Jonson, E.I. Smotrova, A.I. Nosich, V. Korenivski, *Opt. Lett.* 36 (2011) 2381.
- [25] Y.V. Gulyaev, P.E. Zilberman, G.M. Mikhailov, S.G. Chigarev, *JETP Lett.* 98 (2013) 742.
- [26] Y.V. Gulyaev, P.E. Zilberman, S.G. Chigarev, *J. Commun. Technol. Electron.* 60 (2015) 411.
- [27] E.A. Vilkov, G.M. Mikhailov, S.A. Nikitov, A.R. Safin, M.V. Logunov, V.N. Korenivskii, S.G. Chigarev, L.A. Fomin, Dynamics of spatially inhomogeneous spin polarization of nonequilibrium conduction electrons in magnetic transitions, *Phys. Solid State* 61 (6) (2019) 941–951.
- [28] E.I. Rashba, *Fiz. Tverd. Tela. Sov. Phys. -Solid State* 2 (1960) 1224.
- [29] E.A. Karashtin, *JETP Lett.* 112 (2020) 122.
- [30] W.C. Koehler, *J. Appl. Phys.* 36 (1965) 1078.
- [31] Y. Ishikawa, G. Shirane, J.A. Tarvin, M. Kohgi, Magnetic excitations in the weak itinerant ferromagnet MnSi, *Phys. Rev. B* 16 (1977) 4956–4970, <http://dx.doi.org/10.1103/PhysRevB.16.4956>, <https://link.aps.org/doi/10.1103/PhysRevB.16.4956>.
- [32] E.A. Karashtin, O.G. Udalov, *J. Exp. Theor. Phys.* 113 (2011) 992.
- [33] E.A. Karashtin, *Phys. Solid State* 62 (2020) 1647.
- [34] Y. Tserkovnyak, A. Brataas, G.E.W. Bauer, Enhanced Gilbert damping in thin ferromagnetic films, *Phys. Rev. Lett.* 88 (2002) 117601, <http://dx.doi.org/10.1103/PhysRevLett.88.117601>, <https://link.aps.org/doi/10.1103/PhysRevLett.88.117601>.
- [35] J. Sinova, S.O. Valenzuela, J. Wunderlich, C.H. Back, T. Jungwirth, Spin hall effects, *Rev. Mod. Phys.* 87 (2015) 1213–1260, <http://dx.doi.org/10.1103/RevModPhys.87.1213>, <https://link.aps.org/doi/10.1103/RevModPhys.87.1213>.
- [36] J.C.R. Sánchez, L. Vila, G. Desfonds, S. Gambarelli, J.P. Attané, J.M. De Teresa, C. Magén, A. Fert, Spin-to-charge conversion using Rashba coupling at the interface between non-magnetic materials, *Nat. Commun.* 4 (2013) 2944.
- [37] G. Tatara, S. Mizukami, Consistent microscopic analysis of spin pumping effects, *Phys. Rev. B* 96 (2017) 064423, <http://dx.doi.org/10.1103/PhysRevB.96.064423>, <https://link.aps.org/doi/10.1103/PhysRevB.96.064423>.
- [38] H. Wang, C. Du, P. Chris Hammel, F. Yang, Spin current and inverse spin hall effect in ferromagnetic metals probed by Y3Fe5O12-based spin pumping, *Appl. Phys. Lett.* 104 (20) (2014) 202405, <http://dx.doi.org/10.1063/1.4878540>.
- [39] J.C. Slonczewski, *J. Magn. Magn. Mater.* 159 (1996) L1.
- [40] L. Berger, Emission of spin waves by a magnetic multilayer traversed by a current, *Phys. Rev. B* 54 (1996) 9353–9358, <http://dx.doi.org/10.1103/PhysRevB.54.9353>, <https://link.aps.org/doi/10.1103/PhysRevB.54.9353>.
- [41] I. Žutić, J. Fabian, S. Das Sarma, Spintronics: fundamentals and applications, *Rev. Mod. Phys.* 76 (2004) 323–410, <http://dx.doi.org/10.1103/RevModPhys.76.323>, <https://link.aps.org/doi/10.1103/RevModPhys.76.323>.
- [42] M. Calvo, *Phys. Rev. B* 19 (1978) 5507.
- [43] V.M. Matveev, E.L. Nagaev, *Sov. Phys. JETP* 42 (1975) 1094.
- [44] N.S. Gusev, A.V. Sadovnikov, S.A. Nikitov, M.V. Sapozhnikov, O.G. Udalov, Manipulation of the Dzyaloshinskii–Moriya interaction in Co/Pt multilayers with strain, *Phys. Rev. Lett.* 124 (2020) 157202, <http://dx.doi.org/10.1103/PhysRevLett.124.157202>, <https://link.aps.org/doi/10.1103/PhysRevLett.124.157202>.
- [45] E.A. Karashtin, D.A. Tatarskiy, *J. Phys.: Condens. Matter* 32 (2020) 095303.
- [46] L. Piraux, S. Dubois, A. Fert, L. Belliard, *Eur. Phys. J. B* 4 (1998) 413.
- [47] J. Bass, W.P. Pratt, Spin-diffusion lengths in metals and alloys, and spin-flipping at metal/metal interfaces: An experimentalist's critical review, *J. Phys.: Condens. Matter* 19 (18) (2007) 183201, <http://dx.doi.org/10.1088/0953-8984/19/18/183201>.